Noisy swimming at low Reynolds numbers

Jörn Dunkel* and Irwin M. Zaid
Rudolf Peierls Centre for Theoretical Physics, University of Oxford, 1 Keble Road, Oxford OX1 3NP, United Kingdom
(Received 30 March 2009; published 5 August 2009)

Small organisms (e.g., bacteria) and artificial microswimmers move due to a combination of active swimming and passive Brownian motion. Considering a simplified linear three-sphere swimmer, we study how the swimmer size regulates the interplay between self-driven and diffusive behavior at low Reynolds number. Starting from the Kirkwood-Smoluchowski equation and its corresponding Langevin equation, we derive formulas for the orientation correlation time, the mean velocity and the mean-square displacement in three space dimensions. The validity of the analytical results is illustrated through numerical simulations. Tuning the swimmer parameters to values that are typical of bacteria, we find three characteristic regimes: (i) Brownian motion at small times, (ii) quasiballistic behavior at intermediate time scales, and (iii) quasidiffusive behavior at large times due to noise-induced rotation. Our analytical results can be useful for a better quantitative understanding of optimal foraging strategies in bacterial systems, and they can help to construct more efficient artificial microswimmers in fluctuating fluids.

DOI: 10.1103/PhysRevE.80.021903 PACS number(s): 87.17.Jj, 05.40.Jc, 47.63.Gd, 47.63.mf

I. INTRODUCTION

Biological [1–3] and artificial microswimmers [1,4–7] move through a fluid by performing a series of self-induced shape changes [8,9]. Handicapped by their tiny size (typically a few micrometers for a bacterium [10]), they are forced to swim at very low Reynolds numbers $\mathcal{R} \ll 1$ [11–13]. Hence, in order to account for the resulting lack of inertia, the swimming strategies of microorganisms are very different from those operative at human length scales. More precisely, since the fluid flow is reversible at low Reynolds number, locomotion in this regime is possible only if the swimming stroke violates certain time-reversal symmetries [8,13–16].

Stimulated by experimental advances [1–4,17,18], in recent years considerable progress was achieved in understanding the dynamics of deterministic microswimmers models [19–28]. Yet, comparatively little is known quantitatively about the complex interplay between active self-motion, hydrodynamic interactions, and thermal fluctuations in the surrounding fluid [29–32]. Very recently, first steps toward clarifying these issues were made by Howse *et al.* [6], who measured in their experiments the mean square displacement of chemically driven colloidal spheres, and by Lobaskin *et al.* [33], who studied the Brownian motion of a triangular microswimmer at intermediate Reynolds numbers $\mathcal{R} \sim 1$ by combining Lattice Boltzmann simulations with a Langevin description of the swimmer in phase space. In the present paper, we would like to complement these investigations by concentrating on the diffusive properties of mechanically driven microswimmers at low Reynolds numbers $\mathcal{R} \ll 1$. This limit case is most relevant for bacterial motions and allows one to treat diffusive effects within configuration space.

Specifically, we will focus on the following questions: how does the size of the swimmer affect its effective mobility in a noisy fluid? Which details govern the transition from quasiballistic self-motion to the diffusive regime? To shed light on these issues, we shall consider simplified quasilinear p-sphere swimmers similar to those proposed by Najafi and Golestanian [20]. More precisely, we will assume that internal forces, which generate the swimming strokes, are mediated by interaction potentials. This approach permits us to treat thermal diffusion effects within the Kirkwood-Smoluchowski scheme, originally developed to describe the diffusion of polymers in a fluctuating medium [34–37].

Starting from the Kirkwood-Smoluchowski equation (KSE) ensures that hydrodynamic and stochastic forces are consistently coupled on the level of the Fokker-Planck description in configuration space [34]. Moreover, as discussed in Sec. III, the corresponding Langevin equation can be used to derive closed analytical formulas for the orientation correlation time, the mean velocity and the mean square displacement of a single swimmer in three space dimensions. Although the analytical and numerical results in this paper refer to the case of a quasilinear three-sphere swimmer ($p=3$), the formalism can be easily generalized to more complex models (e.g., flexible p-sphere swimmer chains). Therefore, this approach can be generally very useful for studying Brownian motion effects and hydrodynamic interactions in active biological systems at low Reynolds numbers. Furthermore, since it is straightforward to implement an external confinement (e.g., tweezer or lattice potentials), the Kirkwood-Smoluchowski scheme can help to construct and optimize arrays [38] of, e.g., micropumps that work efficiently on those scales where thermal fluctuations in fluid become non-neglible.

Thus, purpose and content of the present paper can be summarized as follows: first, we will discuss a convenient formalism that allows to simulate active microswimming by means of Langevin equations and interaction potentials (Sec. II). Subsequently, we derive analytic results for the diffusion of a single swimmer (Sec. III), thereby extending recent work of Golestanian and Ajdari [25] on deterministic swimmers. A thorough analysis of the single swimmer case is instructive for a number of reasons: (i) Exact analytical re-

*jorn.dunkel@physics.ox.ac.uk

sults provide a useful test of numerical simulations, cf. Sec. IV. (ii) Recently, Leoni *et al.* [4] were able to experimentally realize an individual three-sphere system similar to those considered here. (iii) Understanding the noise-induced behavior of a single swimmer is a prerequisite for understanding complex behavior and pattern formation in, e.g., self-assembling bacterial systems [10]. (iv) Dynamical calculations as those presented below may provide a "microscopic" justification for purely probabilistic models of bacterial motility [39]. (v) Depending on the swimmer size, we find a rather sharp transition from purely Brownian to quasiballistic motions. From a (bio) physical perspective, it is remarkable that the transition occurs when the three-sphere swimmer model is tuned to bacterial parameters. Hence, loosely speaking, exploiting the interplay between Brownian motion and active swimming may indeed represent a useful strategy (not only) in nature.

II. GENERAL THEORETICAL BACKGROUND

We consider an ensemble of N microswimmers, each consisting of p spheres. Neglecting inertia, the state of the system at time t is described by a set of coordinates $(\boldsymbol{X}_\alpha)=\{X_{(\alpha i)}(t)\}$, where $\alpha=1,\ldots,pN$ is a sphere index, and $i=1,2,3$ labels the space dimension. Our subsequent analysis rests on the assumption that the stochastic dynamics of the swimmers in the fluid can be described, at least approximately, by the KSE [34–37], representing evolution for the N-particle probability density $f(t,\{x_{(\alpha i)}\})$. We begin by recalling how the KSE can be translated into a Langevin equation for numerical simulations [36,37]. Details of the swimming mechanism will be discussed in Sec. II B.

A. Kirkwood-Smoluchowski and Langevin equation

Considering a fluid of viscosity μ and temperature $\mathcal{T}$, the KSE reads [34]

$$\partial_t f = \partial_{(\alpha i)}\mathcal{H}_{(\alpha i)(\beta j)}\{[\partial_{(\beta j)}U]f + k_B\mathcal{T}\partial_{(\beta j)}f\}. \tag{1}$$

Here, k_B denotes the Boltzmann constant, $\partial_{(\alpha i)}:=\partial/\partial x_{(\alpha i)}$, and a sum is performed over equal double indices (αi). The (effective [34]) potential U governs all the internal and external swimmer interactions (see examples in Sec. II B), apart from the hydrodynamic interactions mediated by the fluid. The latter are included in the tensor $\mathcal{H}$. Considering spherical particles of radius a_α, the "diagonal" components of $\mathcal{H}$ are given by

$$\mathcal{H}_{(\alpha i)(\alpha j)} = \frac{\delta_{ij}}{\gamma_\alpha}, \quad \gamma_\alpha = 6\pi\mu a_\alpha, \tag{2a}$$

where δ_{ij} denotes the Kronecker symbol, and γ_α is the Stokes friction coefficient. The hydrodynamic interactions between different spheres are encoded in the "off-diagonal" components $\mathcal{H}_{(\alpha i)(\beta j)}$, $\alpha\neq\beta$. If these hydrodynamic interactions are neglected, corresponding to the (infinitely dilute) limit case $\mathcal{H}_{(\alpha i)(\beta j)}=0$, Eq. (1) reduces to an "ordinary" Smoluchowski equation with a diffusion constant $\mathcal{D}_\alpha=k_B\mathcal{T}/\gamma_\alpha$ for each sphere.

Here, we are interested in the effects of hydrodynamic interactions, corresponding to $\mathcal{H}_{(\alpha i)(\beta j)}\neq 0$. A simple approximation for $\mathcal{H}_{(\alpha i)(\beta j)}$, obtained by solving the Stokes equation for a pointlike source, is the Oseen tensor [40,41]

$$\mathcal{H}^O_{(\alpha i)(\beta j)} = \frac{1}{8\pi\mu r_{\alpha\beta}}\left(\delta_{ij}+\frac{r_{\alpha\beta i}r_{\alpha\beta j}}{r^2_{\alpha\beta}}\right), \quad \alpha\neq\beta, \tag{2b}$$

where $r_{\alpha\beta i}:=x_{\alpha i}-x_{\beta i}$ and $r_{\alpha\beta}:=|\boldsymbol{x}_\alpha-\boldsymbol{x}_\beta|$. However, the associated diffusion tensor $D^O:=k_B\mathcal{T}\mathcal{H}^O$ is not necessarily positive definite, leading to unphysical behavior if sphere separations become too small [42,43]. In our numerical simulations we shall therefore use the improved approximation

$$\mathcal{H}^M_{(\alpha i)(\beta j)} = \mathcal{H}^O_{(\alpha i)(\beta j)} + \frac{(a^2_\alpha+a^2_\beta)}{24\pi\mu r^3_{\alpha\beta}}\left(\delta_{ij}-3\frac{r_{\alpha\beta i}r_{\alpha\beta j}}{r^2_{\alpha\beta}}\right), \tag{2c}$$

which was derived by Mazur [44]. The additional term on the right-hand side of Eq. (2c) can be understood as the next-order correction in a radius-over-distance expansion of the mobility tensor for two spheres [45]. For spheres of equal size $(a_\alpha=a_\beta)$, the tensor $\mathcal{H}=\mathcal{H}^M$ defined by Eqs. (2a) and (2c), reduces to the Rotne-Prager-Yamakawa tensor [43,46]. While Eq. (2c) gives a more accurate description than Eq. (2b) at moderate densities, both expressions become invalid if the distance between spheres becomes very small. At very high densities, when sphere-sphere collisions dominate the dynamics, near-field hydrodynamics and lubrication effects must be modeled more carefully [47]. In the present paper, however, we focus on systems that can be described by Eq. (2c).

Unlike the Oseen tensor $\mathcal{H}^O$ from Eq. (2b), the tensor $\mathcal{H}=\mathcal{H}^M$ is positive definite for $r_{\alpha\beta}>a_\alpha+a_\beta$ and thus can be Cholesky decomposed in the form

$$\mathcal{H}_{(\alpha i)(\beta j)} = \frac{1}{2}C_{(\alpha i)(\gamma k)}C_{(\beta j)(\gamma k)}. \tag{3}$$

The decomposition Eq. (3) is crucial if one wishes to find a Langevin representation for the stochastic process $\{X_{(\alpha i)}(t)\}$ described by the KSE Eq. (1): upon noting that [36,48]

$$\partial_{(\alpha i)}\mathcal{H}_{(\alpha i)(\beta j)} \equiv 0 \tag{4}$$

holds (for both $\mathcal{H}^O$ and $\mathcal{H}^M$), one finds that the KSE Eq. (1) corresponds to the following Ito-Langevin equation [49]

$$\mathrm{d}X_{(\alpha i)}(t) = \mathcal{H}_{(\alpha i)(\beta j)}F_{(\beta j)}\mathrm{d}t + (k_B\mathcal{T})^{1/2}C_{(\alpha i)(\gamma k)}\mathrm{d}B_{(\gamma k)}(t). \tag{5}$$

Here, $\{F_{(\beta j)}\}:=\{-\partial_{(\beta j)}U\}$ comprises the deterministic forces acting on the spheres, and $\{B_{(\gamma k)}(t)\}$ is a collection of standard Wiener processes; i.e., the increments $\mathrm{d}B_{(\gamma k)}(t):=B_{\gamma k}(t+\mathrm{d}t)-B_{(\gamma k)}(t)$ are independent GAUSSIAN random numbers with distribution

$$\mathcal{P}\{\mathrm{d}B_{(\gamma k)}(t)\in[u,u+\mathrm{d}u]\} = \frac{e^{-u^2/(2\mathrm{d}t)}}{(2\pi\mathrm{d}t)^{1/2}}\mathrm{d}u, \tag{6}$$

and, according to the Ito scheme [49], the coefficients $C_{(\alpha i)(\gamma k)}$ are to be evaluated at time t. For completeness, we still note that, upon formally dividing by $\mathrm{d}t$, the stochastic

differential Eq. (5) can be rewritten as a "standard" Langevin equation

$$\dot{X}_{(\alpha i)}(t) = \mathcal{H}_{(\alpha i)(\beta j)} F_{(\beta j)} + (k_B \mathcal{T})^{1/2} C_{(\alpha i)(\gamma k)} \xi_{(\gamma k)}(t), \quad (7a)$$

where $\dot{X}_{(\alpha i)}(t) := \mathrm{d}X_{(\alpha i)}(t)/\mathrm{d}t$ denotes the velocity, and $\xi_{(\gamma k)}(t) := \mathrm{d}B_{(\gamma k)}(t)/\mathrm{d}t$ represents GAUSSIAN white noise, i.e.,

$$\langle \xi_{(\alpha i)}(t) \rangle = 0, \quad (7b)$$

$$\langle \xi_{(\alpha i)}(t) \xi_{(\beta j)}(t') \rangle = \delta_{\alpha\beta} \delta_{ij} \delta(t - t'). \quad (7c)$$

B. Swimming mechanism

Having discussed how to implement fluctuations, we still need to specify the swimming mechanism. To this end, consider two spheres α and β that form the leg of a swimmer. We assume that the internal forces between beads α and β, which generate the swimming stroke, can be derived from a time-dependent potential of the form

$$U_{\mathrm{leg}}(t, d_{\alpha\beta}) = \frac{k_0}{2} \{ d_{\alpha\beta} - [\ell + \lambda_{\alpha\beta} \sin(\omega t + \varphi_{\alpha\beta})] \}^2, \quad (8a)$$

with $d_{\alpha\beta}(t) := |\boldsymbol{X}_\alpha(t) - \boldsymbol{X}_\beta(t)|$ denoting the distance between the spheres, $\lambda_{\alpha\beta}$ the approximate amplitude of the stroke, and $\ell > a_\alpha + a_\beta + \lambda_{\alpha\beta}$ the mean length of the leg. The potential U_{leg} gives rise to two characteristic time scales: the driving period $T_\omega := 2\pi/\omega$ and, for a sphere of mass M_α, the oscillator period $T_0 := 2\pi/\sqrt{k_0/M_\alpha}$. Since we are interested in the overdamped regime, these time scales must be long compared to the characteristic damping time $T_\gamma := M_\alpha/\gamma_\alpha$. More precisely, we have to impose

$$T_\gamma \ll T_0 \ll T_\omega \quad (8b)$$

corresponding to slow driving and fast relaxation. The constraint Eq. (8b) ensures that our swimmers behave similar to a shape-driven swimmer [25].

In the remainder, we shall focus on three-sphere swimmers, representing the smallest self-swimming system within our approach (two-sphere swimmers can achieve active locomotion only due to collective effects [16]). We consider three spheres (α, β, γ) forming a swimmer with central sphere β, e.g., in the case of a single swimmer $(\alpha, \beta, \gamma) = (1, 2, 3)$ with middle sphere $\beta = 2$. The legs are given by $\boldsymbol{d}_{\alpha\beta} := \boldsymbol{X}_\beta - \boldsymbol{X}_\alpha$ and $\boldsymbol{d}_{\beta\gamma} := \boldsymbol{X}_\gamma - \boldsymbol{X}_\beta$, and we still define normalized connectors

$$\boldsymbol{n}_{\alpha\beta} := \boldsymbol{d}_{\alpha\beta}/d_{\alpha\beta}, \quad \boldsymbol{n}_{\beta\gamma} := \boldsymbol{d}_{\beta\gamma}/d_{\beta\gamma}.$$

In order to ensure that the swimmer moves quasilinearly [25], we introduce a stiffness potential

$$U_{\mathrm{lin}} = \frac{K}{2} \ell^2 (\boldsymbol{n}_{\alpha\beta} \cdot \boldsymbol{n}_{\beta\gamma} - 1)^2, \quad (9)$$

which, for $K \gg k_0$, penalizes bending. The resulting force components $F^{\mathrm{lin}}_{(\alpha i)} := -\partial_{(\alpha i)} U_{\mathrm{lin}}$ read explicitly

$$F^{\mathrm{lin}}_{\alpha k} = -\frac{Q}{d_{\alpha\beta}} (\delta_{ik} - n_{\alpha\beta i} n_{\alpha\beta k}) n_{\beta\gamma i}, \quad (10a)$$

$$F^{\mathrm{lin}}_{\gamma k} = \frac{Q}{d_{\beta\gamma}} (\delta_{ik} - n_{\beta\gamma i} n_{\beta\gamma k}) n_{\alpha\beta i}, \quad (10b)$$

$$F^{\mathrm{lin}}_{\beta k} = -(F^{\mathrm{lin}}_{\alpha k} + F^{\mathrm{lin}}_{\gamma k}) \quad (10c)$$

where $n_{\alpha\beta i} := d_{\alpha\beta i}/d_{\alpha\beta}$, and

$$Q := K \ell^2 (\boldsymbol{n}_{\alpha\beta} \cdot \boldsymbol{n}_{\beta\gamma} - 1). \quad (10d)$$

Equations (8) and (9) provide a convenient way of modeling and simulating rigid or flexible p-sphere swimmers by means of potentials. We note that, by construction, the sum over the internal swimmer forces is zero. The total potential U appearing in the KSE Eq. (1) is obtained by summing over all effective interaction potentials Eqs. (8) and (9).

III. ANALYTICAL RESULTS

We next summarize formulae for the correlation time of the orientation vector, the mean swimmer velocity and the spatial mean square displacement of an isolated three-sphere swimmer. These analytical results can be obtained from the Langevin Eq. (5) by using the Oseen approximation $\mathcal{H} \simeq \mathcal{H}^O$, and their explicit derivation is discussed in the Appendix.

A swimmer's motion can be characterized by its geometric center

$$\boldsymbol{R}(t) := \frac{1}{3} (\boldsymbol{X}_1 + \boldsymbol{X}_2 + \boldsymbol{X}_3) \quad (11a)$$

and the orientation vector

$$\boldsymbol{N}(t) := \frac{\boldsymbol{X}_3 - \boldsymbol{X}_1}{|\boldsymbol{X}_3 - \boldsymbol{X}_1|}. \quad (11b)$$

We are interested in determining the mean square displacement

$$\mathcal{D}_R(t) := \langle [\boldsymbol{R}(t) - \boldsymbol{R}(0)]^2 \rangle, \quad (12a)$$

and the correlation function

$$\mathcal{D}_N(t) := \langle \boldsymbol{N}(t) \boldsymbol{N}(0) \rangle, \quad (12b)$$

where the average is taken over fluctuations in the fluid (i.e., over all realizations of the Wiener process).

It is convenient to discuss $\mathcal{D}_N(t)$ first. For a deterministic initial state $\boldsymbol{N}(0) = [N_k(0)]$, we can write $\mathcal{D}_N(t) = \langle N_k(t) \rangle N_k(0)$ with a summation over equal indices. To obtain an analytical formula for $\langle N_k(t) \rangle$, we assume that Eq. (8b) holds true and that bending is neglible, $K \gg k_0$. Then the swimmer behaves like a stiff, shape-driven Najafi-Golestanian [20] swimmer and we can approximate

$$\boldsymbol{d}_{12} := \boldsymbol{X}_2 - \boldsymbol{X}_1 \simeq \boldsymbol{N} d_{12}, \quad (13a)$$

$$\boldsymbol{d}_{23} := \boldsymbol{X}_3 - \boldsymbol{X}_2 \simeq \boldsymbol{N} d_{23}, \quad (13b)$$

$$\boldsymbol{d}_{13} := \boldsymbol{X}_3 - \boldsymbol{X}_1 \simeq \boldsymbol{N} (d_{12} + d_{23}), \quad (13c)$$

where, cf. Eq. (8a),

$$d_{12} = \ell + \lambda_{12}\sin(\omega t + \varphi_{12}), \tag{13d}$$

$$d_{23} = \ell + \lambda_{23}\sin(\omega t + \varphi_{23}). \tag{13e}$$

Adopting the Oseen approximation $\mathcal{H} \simeq \mathcal{H}^O$, one can derive from the Langevin Eq. (5) the following linear evolution equation (see App. A1)

$$\langle \dot{N}_k \rangle = -\frac{k_B \mathcal{T}}{2\pi\mu d_{13}^3}\left[\frac{2}{3}\left(\frac{d_{13}}{a_1} + \frac{d_{13}}{a_3}\right) - 1\right]\langle N_k \rangle, \tag{14}$$

where $\langle \dot{N}_k \rangle := \langle dN_k(t)/dt \rangle$. The $1/a_\alpha$-parts are contributions to the rotation rate due to noise on the spheres, whereas the $1/d_{13}^3$ contribution is a correction due to hydrodynamic interactions. Equation (14) can be solved exactly. The solution exhibits an exponentially decaying oscillatory behavior due to the periodicity of the swimming stroke d_{13}. However, for $\ell \gg \max\{\lambda_{\alpha\beta}\}$ it suffices to approximate $d_{13} \simeq 2\ell$, yielding an exponential decay $\mathcal{D}_N(t) \simeq \exp(-t/\tau_N)$ with orientation correlation time

$$\tau_N \simeq \left\{\frac{k_B \mathcal{T}}{16\pi\mu\ell^3}\left[\frac{4}{3}\left(\frac{\ell}{a_1} + \frac{\ell}{a_3}\right) - 1\right]\right\}^{-1}. \tag{15}$$

The time parameter τ_N not only determines the temporal correlation of the orientation vector, it also plays an important role for the dynamics of the geometric center $\boldsymbol{R}(t)$. As shown in Appendix, the mean swimmer velocity $\langle \dot{\boldsymbol{R}}(t) \rangle$ is governed by the equation

$$\langle \dot{R}_k \rangle = \frac{A_1}{3}\langle F_{(1k)} \rangle + \frac{A_3}{3}\langle F_{(3k)} \rangle, \tag{16a}$$

where

$$\langle F_{(1k)} \rangle = -\frac{B_3\langle \dot{d}_{12k} \rangle + C\langle \dot{d}_{23k} \rangle}{B_1 B_3 - C^2}, \tag{16b}$$

$$\langle F_{(3k)} \rangle = \frac{C\langle \dot{d}_{12k} \rangle + B_1\langle \dot{d}_{23k} \rangle}{B_1 B_3 - C^2}, \tag{16c}$$

are the noise-averaged internal forces on the first and third sphere (the force on the central sphere can be eliminated by virtue of $F_{(1k)} + F_{(2k)} + F_{(3k)} \equiv 0$), respectively, and

$$\langle \dot{d}_{12k} \rangle = \langle \dot{N}_k \rangle d_{12} + \langle N_k \rangle \dot{d}_{12}, \tag{16d}$$

$$\langle \dot{d}_{23k} \rangle = \langle \dot{N}_k \rangle d_{23} + \langle N_k \rangle \dot{d}_{23} \tag{16e}$$

the mean change in the leg vectors due stochastic rotations and swimming strokes, with abbreviations

$$A_1 := \frac{1}{\gamma_1} - \frac{1}{\gamma_2} + \frac{1}{4\pi\mu}\left(\frac{1}{d_{13}} - \frac{1}{d_{23}}\right), \tag{16f}$$

$$A_3 := \frac{1}{\gamma_3} - \frac{1}{\gamma_2} + \frac{1}{4\pi\mu}\left(\frac{1}{d_{13}} - \frac{1}{d_{12}}\right), \tag{16g}$$

$$B_1 := \frac{1}{\gamma_1} + \frac{1}{\gamma_2} - \frac{1}{2\pi\mu d_{12}}, \tag{16h}$$

$$B_3 := \frac{1}{\gamma_2} + \frac{1}{\gamma_3} - \frac{1}{2\pi\mu d_{23}}, \tag{16i}$$

$$C := \frac{1}{\gamma_2} - \frac{1}{4\pi\mu}\left(\frac{1}{d_{12}} + \frac{1}{d_{23}} - \frac{1}{d_{13}}\right). \tag{16j}$$

Since the quantities $\langle N_k \rangle$, $\langle \dot{N}_k \rangle$, $d_{\alpha\beta}$, and $\dot{d}_{\alpha\beta}$ are known, Eqs. (16) provide a closed analytical result for the mean velocity $\langle \dot{R}_k \rangle$ of a shape-driven swimmer (within the Oseen approximation). In particular, Eqs. (16) generalize the corresponding velocity formulas for a deterministic swimmer, recently obtained by Golestanian and Ajdari [25], to the "noisy swimming" regime.

For realistic swimmer parameters the orientation correlation time τ_N is typically much larger than the driving period $T_\omega = 2\pi/\omega$. In this case, the rather lengthy result Eq. (16) can be considerably simplified (see last part of App. A2a for details) to read

$$\langle \dot{\boldsymbol{R}}(t) \rangle = \bar{\mathcal{V}}\langle \boldsymbol{N}(t) \rangle. \tag{17a}$$

Here, $\bar{\mathcal{V}}$ denotes the stroke-averaged velocity (i.e, over an interval $[t, t+T_\omega]$) of the corresponding *deterministic* swimmer [25]. By using the approximation Eq. (17a) instead of the exact results Eq. (16) one neglects mean velocity oscillations on small time scales. For example, when considering equal-sized beads with $a_\alpha = a$ and $\ell \gg \max\{a, \lambda_{\alpha\beta}\}$, then

$$\bar{\mathcal{V}} = \frac{7}{24}a\omega\left(\frac{\lambda_{12}\lambda_{23}}{\ell^2}\right)\sin\Delta\varphi, \tag{17b}$$

where $\Delta\varphi := \varphi_{12} - \varphi_{23}$ is the phase difference of the leg contractions, and higher-order terms in a and $\lambda_{\alpha\beta}$ are neglected. Integrating Eq. (17) with $\langle \boldsymbol{N}(t) \rangle \simeq \boldsymbol{N}(0)\exp(-t/\tau_N)$, we obtain for the position mean value of the swimmer the simple approximate result

$$\langle \boldsymbol{R}(t) \rangle \simeq \boldsymbol{R}(0) + \bar{\mathcal{V}}\tau_N[1 - \exp(-t/\tau_N)]\boldsymbol{N}(0); \tag{18}$$

i.e., in the asymptotic limit $t \to \infty$,

$$\langle \boldsymbol{R}(\infty) \rangle = \boldsymbol{R}(0) + \bar{\mathcal{V}}\tau_N \boldsymbol{N}(0). \tag{19}$$

Finally, let us still consider the mean-square displacement $\mathcal{D}_R(t) := \langle [\boldsymbol{R}(t) - \boldsymbol{R}(0)]^2 \rangle$ for a stiff, shape-driven three-sphere swimmer described by Eqs. (13). As discussed in App. A2b, by starting from the Langevin equation for $\boldsymbol{R}(t)$, one can show that $\mathcal{D}_R(t)$ decomposes into the form

$$\mathcal{D}_R(t) = \mathcal{D}_R^{\mathrm{p}}(t) + \mathcal{D}_R^{\mathrm{a}}(t), \tag{20a}$$

where the first part

$$\mathcal{D}_R^{\mathrm{p}}(t) = \frac{1}{9}\frac{k_B\mathcal{T}}{\pi\mu}\left(\frac{1}{a_1} + \frac{1}{a_2} + \frac{1}{a_3}\right)t + \frac{2}{9}\frac{k_B\mathcal{T}}{\pi\mu}\int_0^t \times ds\left(\frac{1}{d_{12}} + \frac{1}{d_{23}} + \frac{1}{d_{13}}\right) \tag{20b}$$

comprises *passive* Brownian motion contributions due to thermal diffusion of the spheres (first line) and hydrodynamic Oseen interactions between them (second line), while the second part

$$\mathcal{D}_R^{\mathrm{a}}(t) \simeq \overline{\mathcal{V}}^2 \int_0^t \mathrm{d}s \int_0^t \mathrm{d}u \langle \boldsymbol{N}(s)\boldsymbol{N}(u)\rangle \tag{20c}$$

is the contribution due to *active* self-swimming. Similar to Eq. (17), the expression Eq. (20c) is valid if the orientation correlation time is much larger than the stroke period, $\tau_N \gg T_\omega$. Inserting the above result $\langle \boldsymbol{N}(t)\boldsymbol{N}(s)\rangle \simeq \exp(-t/\tau_N)$ and approximating $d_{12}=d_{23}=d_{13}/2\simeq \ell$, we obtain for the spatial mean-square displacement

$$\mathcal{D}_R(t) \simeq \frac{1}{9}\frac{k_B\mathcal{T}}{\pi\mu}\left(\frac{1}{a_1}+\frac{1}{a_2}+\frac{1}{a_3}+\frac{5}{\ell}\right)t + 2\overline{\mathcal{V}}^2\tau_N[t+\tau_N(e^{-t/\tau_N}-1)]. \tag{21}$$

The approximate result Eq. (21) provides a coarse-grained stroke-averaged description of the translational diffusion (details of the swimming stroke are encoded in $\overline{\mathcal{V}}$). An analogous formula can be used to describe the diffusion of a spherical, chemically driven microswimmer [6]. By virtue of Eq. (21), we can readily distinguish three distinct regimes:

(i) For $t \ll \tau_N$ we can expand the exponential term to linear order and find

$$\mathcal{D}_R(t) \simeq \mathcal{D}_R^{\mathrm{p}}(t), \tag{22a}$$

i.e., passive Brownian motion dominates on very short time scales.

(ii) For $t \lesssim \tau_N$ we need to include terms quadratic in t/τ_N and obtain

$$\mathcal{D}_R(t) \simeq \mathcal{D}_R^{\mathrm{p}}(t) + \frac{\overline{\mathcal{V}}^2 t^2}{\tau_N}, \tag{22b}$$

i.e., ballistic motion can dominate on intermediate time scales provided $\overline{\mathcal{V}}^2/\tau_N$ is large enough (cf. examples below).

(iii) For $t \gg \tau_N$, we recover diffusive behavior

$$\lim_{t\to\infty}\frac{\mathcal{D}_R(t)}{t} = \frac{\mathcal{D}_R^{\mathrm{p}}(t)}{t} + 2\overline{\mathcal{V}}^2\tau_N. \tag{22c}$$

If the swimmer is constructed such that $2\overline{\mathcal{V}}^2\tau_N \gg \mathcal{D}_R^{\mathrm{p}}(t)/t$, then its diffusive behavior at large times is due to noise-induced rotation (with persistence time τ_N).

In a sense, the above results provide a "microscopic" justification for the assumptions made by Lovely and Dahlquist [39], who studied purely probabilistic models of bacterial motion. We also note that the asymptotic behavior for $t \gg \tau_N$ and $2\overline{\mathcal{V}}^2\tau_N \gg \mathcal{D}_R^{\mathrm{p}}(t)/t$ agrees qualitatively with results reported by Lobaskin *et al.* [33] for triangular swimmers in the moderate Reynolds number regime $\mathcal{R}\sim 1$. In this context, we also mention recent work by Golestanian *et al.* [50], who discuss similar scaling relations for the diffusion of phoretic swimmers.

In the remainder, we are going to compare the analytical predictions with results of computer simulations, based on a direct numerical integration of the Langevin Eq. (5) for the spheres. Our main focus is on the transition from the passive Brownian motions to the active swimming regime.

IV. SWIMMER TUNING & NUMERICAL SIMULATIONS

We simulate a single three-sphere swimmer described by the interaction potentials Eqs. (8) and (9) and governed by the Langevin Eq. (5). We consider identical spheres of radius $a_\alpha=a$, mass $M_\alpha=M$, and equal stroke amplitudes $\lambda_{12}=\lambda_{23}=\lambda$. The density of the spheres is chosen as $\rho=10^3$ kg/m^3 (water), and the fluid is water at room temperature [$\mu=10^{-3}$ kg/(ms), $T=300$ K]. By fixing the parameters of the spring and bending potentials as $k_0=10^{-4}$ kg/s^2, $\omega=10^3$ Hz, and $K=10k_0$, we satisfy the time scale condition Eq. (8b) while ensuring that the swimmer behaves approximately stiff and shape-driven. The velocity $\overline{\mathcal{V}}$ of the swimmer is optimized by choosing $\Delta\varphi=\pi/2$, cf. Eq. (23a).

We are primarily interested in understanding how a change in the swimmer size may affect the diffusive behavior. We therefore fix the ratios $\ell/a=\ell/\lambda=10$ and only vary the leg length ℓ from 1 to 10 μm in our simulations (i.e., the mean swimmer length is $\Lambda=2\ell$). Put differently, we scale the swimmer proportionally by varying ℓ. Having specified all parameters, it is useful to summarize the relevant formulae for our choice

$$\overline{\mathcal{V}} \simeq \frac{7}{24}a\omega\left(\frac{\lambda^2}{\ell^2}\right)\sin\Delta\varphi = 0.292\frac{\ell}{\mathrm{s}}, \tag{23a}$$

$$\tau_N \simeq \frac{16\pi\mu\ell^3}{k_B\mathcal{T}}\left(\frac{8\ell}{3a}-1\right)^{-1} = 0.473\frac{\ell^3\mathrm{s}}{\mu\mathrm{m}^3}, \tag{23b}$$

$$\frac{\mathcal{D}_R^{\mathrm{p}}}{t} \simeq \frac{1}{9}\frac{k_B\mathcal{T}}{\pi\mu}\left(\frac{3}{a}+\frac{5}{\ell}\right) = 5.127\frac{\mu\mathrm{m}^3}{\ell\mathrm{s}}, \tag{23c}$$

and

$$2\overline{\mathcal{V}}^2\tau_N = 0.080\frac{\ell^5}{\mu\mathrm{m}^3\mathrm{s}}. \tag{23d}$$

It is remarkable that increasing the swimmer size by one order of magnitude increases the orientation correlation time τ_N by three orders of magnitude.

Figures 1 and 2 depict the results of numerical simulations (symbols) of the Langevin Eq. (5) and also the corresponding theoretical predictions (dashed lines). The numerical data points represent averages over 100 trajectories with identical initial conditions. More precisely, at time $t=0$ the swimmer is pointing along the x_3 axis with the first sphere being located at the origin, i.e., $\boldsymbol{X}_1(0)=\boldsymbol{0}$, $\boldsymbol{X}_2(0)=\ell\boldsymbol{N}(0)$, and $\boldsymbol{X}_3(0)=[2\ell-\lambda\sin(\Delta\varphi)]\boldsymbol{N}(0)$, where $\boldsymbol{N}(0)=(0,0,1)$.

As evident from the diagrams in Figs. 1 and 2, the results of the numerical simulations are very well matched by the theoretical curves over several orders of magnitude in time. In particular, for a leg length in the range $\ell\sim 5$ μm (red "+"/green "×" symbols) one readily observes the three aforementioned regimes: (i) Brownian diffusion at small time scales $t\ll\tau_N$, (ii) ballistic behavior at intermediate time scales, and (iii) quasidiffusive behavior due to noise-induced rotation for $t\gg\tau_N$.

We conclude the discussion of the numerical results by addressing a few technical aspects that might be relevant and helpful for future simulations. When considering ensembles

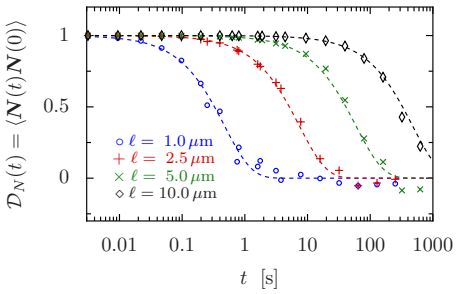

FIG. 1. (Color online) Orientation correlation function for four different swimmer sizes 2ℓ. Symbols represent averages over 100 trajectories, numerically calculated from the Langevin Eq. (5) using parameters as described in the text. The dashed lines depict the theoretically predicted exponential decay $\mathcal{D}_N(t) \simeq \exp(-t/\tau_N)$ with orientation correlation time τ_N determined by Eq. (15). It is remarkable that changing the swimmer size by one order of magnitude increases the correlation time by three orders of magnitude.

with $N > 1$ swimmers the computationally most expensive step is the Cholesky decomposition of the diffusion tensor, see Eq. (3), which is approximately of the order $\mathcal{O}[(pN)^3]$ [36]. It is also worthwhile to briefly comment on the choice of the time step dt in the Langevin simulations. Ideally, one would like to choose dt smaller than the smallest dynamical time scale in the system, which for our model is given by the damping time $T_\gamma = M/(6\pi\mu a)$. For the swimmer parameters considered here we find $T_\gamma \sim 2\times 10^{-9}(\ell/\mu\text{m})^2$s, which means that adopting $dt \sim T_\gamma$ would not allow us to simulate experimentally accessible time scales in the seconds range. Since we are not interested in the dynamical details at very short times scales, we choose in our simulations the time step larger than T_γ, but much smaller than the period T_ω of a swimming stroke by fixing $dt = 10^{-3}T_\omega$ for $\ell < 5$ μm and $dt = 10^{-2}T_\omega$ if $\ell \geq 5$ μm. We verified, however, that for intermediate time scales (of the order of a few stroke periods $T_\omega \sim 6\times 10^{-3}$ s) the numerical results for the mean square

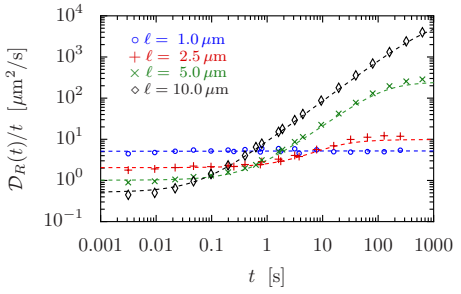

FIG. 2. (Color online) Mean-square displacement $\mathcal{D}_R(t) := \langle [\boldsymbol{R}(t) - \boldsymbol{R}(0)]^2 \rangle$ divided by time t for the same set of parameters as in Fig. 1. The dashed lines correspond to the analytical formula (21). The dynamics of small swimmers ($\ell = 1$ μm, blue circles) is dominated by Brownian motion on all time scales, whereas big swimmers ($\ell = 10$ μm, black diamonds) can move ballistically for several minutes. In the intermediate region ($\ell \sim 5$ μm, red "+"/green "×") we observe a ballistic transition from ordinary Brownian motion at small times $t \ll \tau_N$ to noise-induced rotational diffusion at large times $t \gg \tau_N$. Since $\tau_N \sim \ell^3$, the transition from Brownian to quasiballistic motion is very sharp. Interestingly enough, typical sizes of bacteria lie in or near this niche [10].

displacement and other statistical observables agree with those obtained for very small time steps $dt = 0.1T_\gamma$. Generally, a satisfactory resolution of the bending and relaxation dynamics of the legs/spheres would require $dt \ll (M/K)^{1/2}$ and $dt \ll (M/k_0)^{1/2}$, respectively.

V. CONCLUSIONS

Understanding the interplay between Brownian motion, hydrodynamic interactions, and self-propulsion is a prerequisite for understanding the dynamics of bacteria and artificial swimming devices at the microscale. In the first part, we discussed how one can model these phenomena by means of stochastic processes (overdamped Langevin equations). Subsequently, as a first application, we focused on the size dependence of diffusive behavior at low Reynolds numbers ($\mathcal{R} \ll 1$) for a quasilinear three-sphere swimmer model. Our theoretical analysis complements a recent experimental study by Howse *et al.* [6], who investigated the diffusion of chemically driven, spherical colloids, and theoretical work by Lobaskin *et al.* [33], who considered the Brownian dynamics of an artificial triangular microswimmer at moderate Reynolds numbers ($\mathcal{R} \sim 1$).

Starting from the Kirkwood-Smoluchowski equation [34–37], we derived analytical results for the orientation correlation time, the mean velocity, and the mean-square displacement of an overdamped, quasilinear three-sphere swimmer [20,25]. Analytical formulae as derived here are useful for testing numerical simulations and (in) validating simplified probabilistic models [39]. Moreover, they provide detailed insight into the size-regulated transition from predominantly random to quasiballistic motions.

The proposed method of modeling swimmers by effective potentials within a Langevin scheme can be readily extended to study complex behavior in larger swimmer ensembles. However, at high swimmer densities, collisions, and near-field hydrodynamics affect the diffusive behavior [47,51,52] and it will be necessary to modify the hydrodynamic interaction tensor accordingly. Generally, a useful dimensionless quantifier for the efficiency of active swimming relative to diffusion is given by the ratio

$$\epsilon = \frac{\tau_N}{\Lambda/\bar{\mathcal{V}}}. \tag{24}$$

The denominator corresponds to the time needed by a unperturbed swimmer of velocity $\bar{\mathcal{V}}$ to move one body length Λ, and the swimmer geometry is encoded in the orientation correlation time τ_N. For $\epsilon \gg 1$ ($\epsilon \ll 1$) self-propulsion is effective (noneffective). For nonisolated swimmers, τ_N is not only determined by thermal effects, but also by collisions with other swimmers [51,52].

With regard to future studies we note that the combination of thermal fluctuations and hydrodynamic coupling might also lead to interesting behavior in simple arrangements of microswimmers. For example, experiments have shown that colloidal spheres localized in an array of optical traps create memory effects [53] and driven vibrations [54]. Our formalism provides a starting point for the investigation of many

self-propelled bodies in separate potentials, which could be helpful for interpreting experimental data of trapped bacteria or for constructing pumps from a collection of microswimmers.

To summarize, the above results may provide guidance for constructing artificial microswimmers or pumps that work efficiently in the critical transition region that separates Brownian from quasideterministic motions. In particular, by tuning the parameters to the narrow cross-over region one could construct swimmers that explore with high probability a maximized volume fraction within a given period of time. The fact that many bacteria live near or exactly in this niche [10] suggest that this may indeed be a useful strategy. Thus, exploiting the interplay between noise and active self-motion could lead to novel applications [55], e.g., with regard to the controlled transport [56] and distribution of chemical and biological substances in small scale technical devices or even within the human body.

ACKNOWLEDGMENTS

The authors would like to thank Matthieu Dufay, Bortolo Mognetti, Olivier Pierre-Louis, Victor Putz, and Julia Yeomans for helpful discussions. This work was supported by the EPSRC grant no. EP/D050952/1 (J.D.).

APPENDIX: CALCULATIONS

This appendix provides derivations of analytical results for the orientation correlation function, the mean velocity, and the spatial mean square displacement from the Langevin Eq. (5). Our calculations are based on the following simplifying assumptions:

(i) The motion of the three-sphere swimmer is approximately stiff and shape-driven, i.e.,

$$\boldsymbol{d}_{12} := \boldsymbol{X}_2 - \boldsymbol{X}_1 \simeq \boldsymbol{N} d_{12}, \tag{A1a}$$

$$\boldsymbol{d}_{23} := \boldsymbol{X}_3 - \boldsymbol{X}_2 \simeq \boldsymbol{N} d_{23}, \tag{A1b}$$

$$\boldsymbol{d}_{13} := \boldsymbol{X}_3 - \boldsymbol{X}_1 \simeq \boldsymbol{N}(d_{12} + d_{23}), \tag{A1c}$$

where

$$d_{12} = \ell + \lambda_{12} \sin(\omega t), \tag{A1d}$$

$$d_{23} = \ell + \lambda_{23} \sin(\omega t - \Delta\varphi). \tag{A1e}$$

In this case the internal forces, which generate the swimming strokes, point along the swimmer's axis and we may write

$$F_{1i} = g_1 N_i, \quad F_{3i} = g_3 N_i \tag{A2a}$$

and, with $F_{3i}+F_{2i}+F_{1i}=0$,

$$F_{2i} = -(g_1 + g_3) N_i, \tag{A2b}$$

where g_α is the force amplitude, and N_i denotes a component of the orientation vector

$$\boldsymbol{N}(t) := \frac{\boldsymbol{X}_3 - \boldsymbol{X}_1}{|\boldsymbol{X}_3 - \boldsymbol{X}_1|}. \tag{A2c}$$

(ii) We adopt the Oseen approximation, i.e., $\mathcal{H} \simeq \mathcal{H}^O$ where

$$\mathcal{H}^O_{(\alpha i)(\beta j)} := \frac{1}{8\pi\mu d_{\alpha\beta}} \left(\delta_{ij} + \frac{d_{\alpha\beta i} d_{\alpha\beta j}}{d^2_{\alpha\beta}} \right),$$

$$\simeq \frac{1}{8\pi\mu d_{\alpha\beta}} (\delta_{ij} + N_i N_j). \tag{A3}$$

The second line follows from assumption Eq. (A1).

1. Orientation correlation function

Given a deterministic initial state $\boldsymbol{N}(0)=[N_k(0)]$, we are interested in $\mathcal{D}_N(t) := \langle \boldsymbol{N}(t)\boldsymbol{N}(0)\rangle = \langle N_k(t)\rangle N_k(0)$.

The first step is to find the stochastic differential equation (SDE) for the orientation vector $\boldsymbol{N}(t)$. This can be achieved by virtue of the Ito formula [49,57], yielding

$$\mathrm{d}N_k(t) = \partial_{(\alpha i)} N_k \mathrm{d}X_{(\alpha i)} + D_{(\alpha i)(\beta j)} \partial_{(\alpha i)} \partial_{(\beta j)} N_k \mathrm{d}t, \tag{A4}$$

where $\mathrm{d}X_{(\alpha i)}(t)$ is governed by Eq. (5), and the diffusion tensor is given by $D := k_B \mathcal{T} \mathcal{H} \simeq k_B \mathcal{T} \mathcal{H}^O$.

To determine $\langle N_k(t)\rangle$, we use that $\langle C_{(\alpha i)(\gamma k)} \mathrm{d}B_{(\gamma k)}(t)\rangle = 0$ for an Ito SDE, and therefore

$$\mathrm{d}\langle X_{(\alpha i)(t)}\rangle = \langle \mathcal{H}_{(\alpha i)(\beta j)} F_{(\beta j)}\rangle \mathrm{d}t. \tag{A5}$$

Taking the average of Eq. (A4) and inserting Eq. (A5), we obtain

$$\langle \dot{N}_k(t)\rangle = \langle \mathcal{H}_{(\alpha i)(\beta j)} F_{(\beta j)} \partial_{(\alpha i)} N_k\rangle + \langle D_{(\alpha i)(\beta j)} \partial_{(\alpha i)} \partial_{(\beta j)} N_k\rangle, \tag{A6}$$

where $\mathrm{d}\langle \dot{N}_k(t)\rangle := \langle \mathrm{d}N_k(t)/\mathrm{d}t\rangle$. We next evaluate the two terms the right-hand side of Eq. (A6) separately. To this end we note that

$$\partial_{(\alpha j)} N_k = \frac{1}{d_{13}} (\delta_{3\alpha} - \delta_{1\alpha})(\delta_{jk} - N_j N_k), \tag{A7}$$

yielding for the first term

$$\mathcal{H}_{(\alpha i)(\beta j)} F_{(\beta j)} \partial_{(\alpha i)} N_k = [\mathcal{H}_{(3i)(\beta j)} - \mathcal{H}_{(1i)(\beta j)}] \times \frac{F_{(\beta j)}}{d_{13}} (\delta_{ik} - N_i N_k). \tag{A8}$$

Using Oseen approximation Eq. (A3), we find

$$\mathcal{H}_{(3i)(\beta j)} F_{(\beta j)} = \left[\frac{g_3}{\gamma_3} + \frac{g_1}{4\pi\mu d_{31}} - \frac{(g_3 + g_1)}{4\pi\mu d_{32}} \right] N_i,$$

and, similarly, $\mathcal{H}_{(1i)(\beta j)} F_{(\beta j)} \propto N_i$. Taking into account that

$$N_i(\delta_{ik} - N_i N_k) \equiv 0, \tag{A9}$$

the first term on the right-hand side of Eq. (A6) vanishes, and Eq. (A6) reduces to

$$\langle \dot{N}_k(t)\rangle = \langle D_{(\alpha i)(\beta j)} \partial_{(\alpha i)} \partial_{(\beta j)} N_k\rangle. \tag{A10}$$

By virtue of Eq. (A7), we find

$$\partial_{(\alpha i)}\partial_{(\beta j)}N_k = \frac{1}{d_{13}^2}(\delta_{3\beta}-\delta_{1\beta})(\delta_{3\alpha}-\delta_{1\alpha}) \times (3N_jN_kN_i - N_j\delta_{ik} - N_k\delta_{ij} - N_i\delta_{jk}). \tag{A11}$$

To obtain the right-hand side of Eq. (A10), we still need to contract with the diffusion tensor $D_{(\alpha i)(\beta j)}$. This results in two contributions: From the diagonal part we get

$$k_B\mathcal{T}\sum_{(\alpha j)}\frac{1}{\gamma_\alpha}(\delta_{3\alpha}-\delta_{1\alpha})(\delta_{3\alpha}-\delta_{1\alpha}) \times \frac{1}{d_{13}^2}(3N_jN_kN_j - N_j\delta_{jk} - N_k\delta_{jj} - N_j\delta_{jk}) = -k_B\mathcal{T}\left(\frac{1}{\gamma_1}+\frac{1}{\gamma_3}\right)\frac{2N_k}{d_{13}^2}, \tag{A12a}$$

while the hydrodynamic off-diagonal terms give

$$k_B\mathcal{T}\sum_{(\alpha i)(\beta j)}(1-\delta_{\alpha\beta})(\delta_{3\alpha}-\delta_{1\alpha})(\delta_{3\beta}-\delta_{1\beta}) \times \frac{(\delta_{ij}+N_iN_j)}{8\pi\mu d_{\alpha\beta}}\frac{1}{d_{13}^2}(3N_iN_kN_j - N_j\delta_{ik} - N_k\delta_{ij} - N_i\delta_{jk}) = \frac{k_B\mathcal{T}}{2\pi\mu d_{13}^3}N_k. \tag{A12b}$$

Combining the two contributions we find

$$\langle\dot{N}_k(t)\rangle = \left[-k_B\mathcal{T}\left(\frac{1}{\gamma_1}+\frac{1}{\gamma_3}\right)\frac{2}{d_{13}^2}+\frac{k_B\mathcal{T}}{2\pi\mu d_{13}^3}\right]\langle N_k\rangle,$$

which for $\gamma_\alpha = 6\pi\mu a_\alpha$ gives Eq. (14).

2. Motion of the geometric center

Following a similar procedure, we can derive analytical expression for the mean velocity $\langle\dot{\boldsymbol{R}}(t)\rangle$ and the mean-square displacement $\mathcal{D}_R(t)$.

a. Mean velocity

First, we would like to determine the mean velocity $\langle\dot{\boldsymbol{R}}(t)\rangle$ of the swimmer's geometric center

$$\boldsymbol{R}(t) := \frac{1}{3}(\boldsymbol{X}_1+\boldsymbol{X}_2+\boldsymbol{X}_3). \tag{A13}$$

Averaging the stochastic differential equation

$$\mathrm{d}\boldsymbol{R}(t) := \frac{1}{3}(\mathrm{d}\boldsymbol{X}_1+\mathrm{d}\boldsymbol{X}_2+\mathrm{d}\boldsymbol{X}_3) \tag{A14}$$

with respect to the underlying Wiener process and dividing by $\mathrm{d}t$, we obtain

$$\langle\dot{R}_i(t)\rangle = \frac{1}{3}\sum_{\alpha=1}^{3}\langle\mathcal{H}_{(\alpha i)(\beta j)}F_{(\beta j)}\rangle = \frac{1}{3}\sum_{\alpha=1}^{3}\left\langle\frac{F_{(\alpha i)}}{\gamma_\alpha}+(1-\delta_{\alpha\beta})\mathcal{H}_{(\alpha i)(\beta j)}F_{(\beta j)}\right\rangle. \tag{A15}$$

Considering as before a stiff, shape-driven swimmer and Oseen interactions $\mathcal{H}=\mathcal{H}^O$, we have $F_{(\beta i)}\simeq g_\beta N_i$ and, therefore,

$$\sum_{\beta\neq\alpha}\mathcal{H}_{(\alpha i)(\beta j)}F_{(\beta j)} \simeq \sum_{\beta\neq\alpha}\frac{(\delta_{ij}+N_iN_j)}{8\pi\mu d_{\alpha\beta}}g_\beta N_j = N_i\sum_{\beta\neq\alpha}\frac{g_\beta}{4\pi\mu d_{\alpha\beta}}. \tag{A16}$$

Inserting this into Eq. (A15) gives

$$\langle\dot{R}_i(t)\rangle = \frac{1}{3}\left\langle N_i\left(\frac{g_1}{\gamma_1}+\frac{g_2}{\gamma_2}+\frac{g_3}{\gamma_3}+\frac{g_2}{4\pi\mu d_{12}}+\frac{g_3}{4\pi\mu d_{13}} +\frac{g_1}{4\pi\mu d_{12}}+\frac{g_3}{4\pi\mu d_{23}}+\frac{g_1}{4\pi\mu d_{13}}+\frac{g_2}{4\pi\mu d_{23}}\right)\right\rangle$$

Since the internal swimming forces sum to zero, we may eliminate g_2 by using $g_2=-(g_1+g_3)$ to obtain

$$\langle\dot{R}_i(t)\rangle = \frac{1}{3}\langle N_ig_1\rangle\left[\frac{1}{\gamma_1}-\frac{1}{\gamma_2}+\frac{1}{4\pi\mu}\left(\frac{1}{d_{13}}-\frac{1}{d_{23}}\right)\right]+\frac{1}{3}\langle N_ig_3\rangle \times\left[\frac{1}{\gamma_3}-\frac{1}{\gamma_2}+\frac{1}{4\pi\mu}\left(\frac{1}{d_{13}}-\frac{1}{d_{12}}\right)\right]$$

$$=: \frac{A_1}{3}\langle N_ig_1\rangle+\frac{A_3}{3}\langle N_ig_3\rangle. \tag{A17}$$

Consequently, to find $\langle\dot{R}_i(t)\rangle$, we still need to determine the mean forces $\langle F_{(\beta i)}\rangle=\langle N_ig_\beta\rangle$ on the first and last sphere, $\beta=1,3$. This can be achieved as follows: Eq. (A1) implies that

$$\langle\dot{d}_{12k}\rangle = \langle\dot{N}_k\rangle d_{12}+\langle N_k\rangle\dot{d}_{12}, \tag{A18a}$$

$$\langle\dot{d}_{23k}\rangle = \langle\dot{N}_k\rangle d_{23}+\langle N_k\rangle\dot{d}_{23}. \tag{A18b}$$

On the other hand, from the definition of the vectors $\boldsymbol{d}_{\alpha\beta}$ and the Langevin equations for $\mathrm{d}\boldsymbol{X}_\alpha$, we have

$$\langle\dot{d}_{12k}\rangle = \langle\mathcal{H}_{(2k)(\beta j)}F_{(\beta j)}-\mathcal{H}_{(1k)(\beta j)}F_{(\beta j)}\rangle, \tag{A19a}$$

$$\langle\dot{d}_{23k}\rangle = \langle\mathcal{H}_{(3k)(\beta j)}F_{(\beta j)}-\mathcal{H}_{(2k)(\beta j)}F_{(\beta j)}\rangle. \tag{A19b}$$

Inserting the explicit expressions for $\mathcal{H}_{(\alpha i)(\beta j)}$ and $F_{(\beta j)}$, Eqs. (A19) can be rewritten as

$$\langle\dot{d}_{12k}\rangle = -\left[\frac{1}{\gamma_1}+\frac{1}{\gamma_2}-\frac{1}{2\pi\mu d_{12}}\right]\langle N_kg_1\rangle - \left[\frac{1}{\gamma_2}-\frac{1}{4\pi\mu}\left(\frac{1}{d_{12}}+\frac{1}{d_{23}}-\frac{1}{d_{13}}\right)\right]\langle N_kg_3\rangle$$

$$=: -B_1\langle N_k g_1\rangle - C\langle N_k g_3\rangle \tag{A20a}$$

and

$$\langle \dot{d}_{23k}\rangle = \left[\frac{1}{\gamma_2} - \frac{1}{4\pi\mu}\left(\frac{1}{d_{12}} + \frac{1}{d_{23}} - \frac{1}{d_{13}}\right)\right]\langle N_k g_1\rangle + \left[\frac{1}{\gamma_2} + \frac{1}{\gamma_3} - \frac{1}{2\pi\mu d_{23}}\right]\langle N_k g_3\rangle$$

$$=: C\langle N_k g_1\rangle + B_3\langle N_k g_3\rangle. \tag{A20b}$$

Hence, in order to obtain the unknown expectation values $\langle N_k g_1\rangle$, we have to solve the linear system

$$\langle \dot{d}_{12k}\rangle = -B_1\langle N_k g_1\rangle - C\langle N_k g_3\rangle, \tag{A21a}$$

$$\langle \dot{d}_{23k}\rangle = C\langle N_k g_1\rangle + B_3\langle N_k g_3\rangle, \tag{A21b}$$

With left-hand side given by Eqs. (A19). This is easily done and we may summarize the result for the mean velocity

$$\langle \dot{R}_k(t)\rangle = \frac{A_1}{3}\langle N_k g_1\rangle + \frac{A_3}{3}\langle N_k g_3\rangle, \tag{A22a}$$

where

$$\langle N_k g_1\rangle = -\frac{B_3\langle \dot{d}_{12k}\rangle + C\langle \dot{d}_{23k}\rangle}{B_1B_3 - C^2}, \tag{A22b}$$

$$\langle N_k g_3\rangle = \frac{C\langle \dot{d}_{12k}\rangle + B_1\langle \dot{d}_{23k}\rangle}{B_1B_3 - C^2}, \tag{A22c}$$

with

$$\langle \dot{d}_{12k}\rangle = \langle \dot{N}_k\rangle d_{12} + \langle N_k\rangle \dot{d}_{12}, \tag{A22d}$$

$$\langle \dot{d}_{23k}\rangle = \langle \dot{N}_k\rangle d_{23} + \langle N_k\rangle \dot{d}_{23}. \tag{A22e}$$

Since the quantities $\langle N_k\rangle$, $\langle \dot{N}_k\rangle$, $d_{\alpha\beta}$, $\dot{d}_{\alpha\beta}$, A_α, B_α, and C are known we have thus obtained a closed analytical result for the mean swimmer velocity within the Oseen approximation. Analogous calculations can be performed for $\mathcal{H}^M$, but do not yield much additional insight (for a single swimmer).

Additional simplifications. If the orientation correlation time τ_N is larger than the driving period $T=2\pi/\omega$ then

$$\langle \dot{d}_{12k}\rangle \simeq \langle N_k\rangle \dot{d}_{12}, \quad \langle \dot{d}_{23k}\rangle \simeq \langle N_k\rangle \dot{d}_{23}. \tag{A23}$$

In this case, we may simplify

$$\langle \dot{R}_k(t)\rangle \simeq \mathcal{V}(t)\langle N_k(t)\rangle, \tag{A24a}$$

where

$$\mathcal{V}(t) = -\frac{A_1}{3}\left(\frac{B_3\dot{d}_{12} + C\dot{d}_{23}}{B_1B_3 - C^2}\right) + \frac{A_3}{3}\left(\frac{C\dot{d}_{12} + B_1\dot{d}_{23}}{B_1B_3 - C^2}\right) \tag{A24b}$$

is a periodic function, $\mathcal{V}(t)=\mathcal{V}(t+T_\omega)$. Since we assumed $\tau_N \gg T_\omega$, we can achieve further simplification by replacing $\mathcal{V}(t)$ with its stroke average

$$\overline{\mathcal{V}} := \int_t^{t+T_\omega} \mathrm{d}s\,\mathcal{V}(s), \tag{A25}$$

so that

$$\langle \dot{R}_k(t)\rangle \simeq \overline{\mathcal{V}}\langle N_k(t)\rangle. \tag{A26}$$

For example, when considering equal-sized beads with $a_\alpha = a$ and $\ell \gg \max\{a, \lambda_{12}, \lambda_{23}\}$, then

$$\mathcal{V}(t) = \frac{a\omega\lambda_{12}}{\ell}\cos(\omega t + \varphi_{12}) + \frac{a\omega\lambda_{23}}{\ell}\cos(\omega t + \varphi_{23}) + \overline{\mathcal{V}},$$

where

$$\overline{\mathcal{V}} = \frac{7}{24}a\omega\left(\frac{\lambda_{12}\lambda_{23}}{\ell^2}\right)\sin\Delta\varphi \tag{A27}$$

and $\Delta\varphi := \varphi_{12} - \varphi_{23}$, and higher-order terms have been neglected.

b. Spatial diffusion

Using the result for $\mathrm{d}R(t)$ from above, we may rewrite the mean square displacement $\mathcal{D}_R(t)$ as

$$\begin{aligned}\mathcal{D}_R(t) &:= \langle [\boldsymbol{R}(t) - \boldsymbol{R}(0)]^2\rangle \\ &= \left\langle \int_0^t \mathrm{d}R_k(u)\int_0^t \mathrm{d}R_k(s)\right\rangle \\ &= \int_0^t \mathrm{d}s\int_0^t \mathrm{d}u\left\langle \left[\frac{A_1}{3}N_k g_1 + \frac{A_3}{3}N_k g_3\right]_s \right. \\ &\quad \left. \times \left[\frac{A_1}{3}N_k g_1 + \frac{A_3}{3}N_k g_3\right]_u\right\rangle \\ &\quad + \frac{1}{9}\sum_{\alpha,\alpha'=1}^{3}\int \langle [C_{(\alpha k)(\gamma n)}]_s \mathrm{d}B_{(\gamma n)}(s) \\ &\quad \times [C_{(\alpha' k)(\gamma' n')}]_u \mathrm{d}B_{(\gamma' n')}(u)\rangle.\end{aligned} \tag{A28}$$

Here, we have again used that $\langle \int f(\boldsymbol{X}_\alpha)\mathrm{d}B_{(\gamma n)}(t)\rangle = 0$ holds for Ito integrals. We consider the two remaining integrals in Eq. (A28) separately, starting with the second one. We find

$$\begin{aligned}\mathcal{D}_R^{\mathrm{p}}(t) &:= \frac{1}{9}\sum_{\alpha,\alpha'=1}^{3}\int \langle [C_{(\alpha k)(\gamma n)}]_s \mathrm{d}B_{(\gamma n)}(s) \\ &\quad \times [C_{(\alpha' k)(\gamma' n')}]_u \mathrm{d}B_{(\gamma' n')}(u)\rangle \\ &= \frac{2}{9}\sum_{\alpha,\alpha'=1}^{3}\int_0^t \mathrm{d}s\langle D_{(\alpha k)(\alpha' k)}\rangle \\ &= \frac{2}{9}k_B\mathcal{T}\int_0^t \mathrm{d}s\left[\frac{3}{\gamma_1} + \frac{3}{\gamma_2} + \frac{3}{\gamma_3}\right] \\ &\quad + \frac{2}{9}k_B\mathcal{T}\sum_{\alpha,\alpha'=1}^{3}(1-\delta_{\alpha\alpha'})\int_0^t \mathrm{d}s\mathcal{H}^O_{(\alpha k)(\alpha' k)},\end{aligned}$$

where

$$\mathcal{H}^{O}_{(\alpha k)(\alpha' k)} = \frac{\delta_{kk} + N_k N_k}{8\pi\mu d_{\alpha\alpha'}} = \frac{1}{2\pi\mu d_{\alpha\alpha'}}. \tag{A29}$$

For spherical particles we have $\gamma_\alpha = 6\pi\mu a_\alpha$ and, therefore,

$$\mathcal{D}^{\mathrm{p}}_R(t) = \frac{1}{9}\frac{k_B\mathcal{T}}{\pi\mu}\left(\frac{1}{a_1}+\frac{1}{a_2}+\frac{1}{a_3}\right)t + \frac{2}{9}\frac{k_B\mathcal{T}}{\pi\mu}\int_0^t \mathrm{d}s\left(\frac{1}{d_{12}}+\frac{1}{d_{23}}+\frac{1}{d_{13}}\right).$$

For $\ell \gg \max\{\lambda_{\alpha\beta}\}$, the integrand in the second line can be approximated by $5/(2\ell)$ yielding

$$\mathcal{D}^{\mathrm{p}}_R(t) \simeq \frac{1}{9}\frac{k_B\mathcal{T}}{\pi\mu}\left(\frac{1}{a_1}+\frac{1}{a_2}+\frac{1}{a_3}+\frac{5}{\ell}\right)t. \tag{A30}$$

It remains to determine the first (double) integral in Eq. (A28), reading

$$\mathcal{D}^{\mathrm{a}}_R(t) := \int_0^t \mathrm{d}s \int_0^t \mathrm{d}u \left\langle \left[\frac{A_1}{3}N_k g_1 + \frac{A_3}{3}N_k g_3\right]_s \times \left[\frac{A_1}{3}N_k g_1 + \frac{A_3}{3}N_k g_3\right]_u \right\rangle.$$

The subscripts indicate the time arguments in the bracketed expressions, respectively. Upon recalling that $F_{(\alpha i)} = g_\alpha N_i$ is the internal force acting on sphere α, we see that the contribution $D^{\mathrm{a}}_R(t)$ is essentially determined by the force-force correlation functions. However, instead of calculating these correlation functions exactly, we may approximate, for $\tau_N \gg T_\omega$, the integrand by [cf. Eqs. (A17) and (A26)]

$$\langle [\ldots]_s [\ldots]_u \rangle \simeq \overline{\mathcal{V}}^2 \langle N_k(s) N_k(u)\rangle,$$

where $\overline{\mathcal{V}}$ is the stroke-averaged velocity of the corresponding deterministic swimmer, cf. Eqs. (A25) and (A26). Adopting this approximation we find

$$\begin{aligned}\mathcal{D}^{\mathrm{a}}_R(t) &\simeq \overline{\mathcal{V}}^2 \int_0^t \mathrm{d}s \int_0^t \mathrm{d}u \langle N_k(s) N_k(u)\rangle \\ &= \overline{\mathcal{V}}^2 \int_0^t \mathrm{d}s \int_0^t \mathrm{d}u \, \exp(-|u-s|/\tau_N) \\ &= 2\overline{\mathcal{V}}^2 \tau_N [t + \tau_N (e^{-t/\tau_N} - 1)],\end{aligned}$$

and thus the final result

$$\begin{aligned}\mathcal{D}_R(t) &= \mathcal{D}^{\mathrm{p}}_R(t) + \mathcal{D}^{\mathrm{a}}_R(t) \\ &\simeq \frac{1}{9}\frac{k_B\mathcal{T}}{\pi\mu}\left(\frac{1}{a_1}+\frac{1}{a_2}+\frac{1}{a_3}+\frac{5}{\ell}\right)t \\ &\quad + 2\overline{\mathcal{V}}^2 \tau_N [t + \tau_N (e^{-t/\tau_N} - 1)].\end{aligned} \tag{A31}$$

The first part represents passive (thermal) diffusion; the second part is due to active swimming (note that τ_N is temperature dependent as well).

[1] R. Dreyfus, J. Baudry, M. L. Roper, M. Fermigier, H. A. Stone, and J. Bibette, Nature (London) **437**, 862 (2005).
[2] A. Sokolov, I. S. Aranson, J. O. Kessler, and R. E. Goldstein, Phys. Rev. Lett. **98**, 158102 (2007).
[3] A. P. Berke, L. Turner, H. C. Berg, and E. Lauga, Phys. Rev. Lett. **101**, 038102 (2008).
[4] M. Leoni, J. Kotar, B. Bassetti, P. Cicuta, and M. C. Lagomarsino, Soft Matter **5**, 472 (2009).
[5] P. Tierno, R. Golestanian, I. Pagonabarraga, and F. Sagues, J. Phys. Chem. B. **112**, 16525 (2008).
[6] J. R. Howse, R. A. L. Jones, A. J. Ryan, T. Gough, R. Vafabakhsh, and R. Golestanian, Phys. Rev. Lett. **99**, 048102 (2007).
[7] P. Tierno, R. Golestanian, I. Pagonabarraga, and F. Sagues, Phys. Rev. Lett. **101**, 218304 (2008).
[8] A. Shapere and F. Wilczek, J. Fluid Mech. **198**, 557 (1989).
[9] H. A. Stone and A. D. T. Samuel, Phys. Rev. Lett. **77**, 4102 (1996).
[10] M. F. Copeland and D. B. Weibel, Soft Matter **5**, 1174 (2009).
[11] O. Reynolds, Philos. Trans. R. Soc. Lond. **174**, 935 (1883).
[12] J. Lighthill, SIAM Rev. **18**, 161 (1976).
[13] E. M. Purcell, Am. J. Phys. **45**, 3 (1977).
[14] J. Koiller, K. Ehlers, and R. Montgomery, J. Nonlinear Sci. **6**, 507 (1996).
[15] E. Yariv, J. Fluid Mech. **550**, 139 (2006).
[16] E. Lauga and D. Bartolo, Phys. Rev. E **78**, 030901(R) (2008).
[17] H. C. Berg, Phys. Today **53**(1), 24 (2000).
[18] C. Dombrowski, L. Cisneros, S. Chatkaew, R. E. Goldstein, and J. O. Kessler, Phys. Rev. Lett. **93**, 098103 (2004).
[19] L. E. Becker, S. A. Koehler, and H. A. Stone, J. Fluid Mech. **490**, 15 (2003).
[20] A. Najafi and R. Golestanian, Phys. Rev. E **69**, 062901 (2004).
[21] T. Ishikawa, G. Sekiya, Y. Imai, and T. Yamaguchi, Biophys. J. **93**, 2217 (2007).
[22] D. J. Earl, C. M. Pooley, J. F. Ryder, I. Bredberg, and J. M. Yeomans, J. Chem. Phys. **126**, 064703 (2007).
[23] C. M. Pooley, G. P. Alexander, and J. M. Yeomans, Phys. Rev. Lett. **99**, 228103 (2007).
[24] G. P. Alexander and J. Yeomans, Europhys. Lett. **83**, 34006 (2008).
[25] R. Golestanian and A. Ajdari, Phys. Rev. E **77**, 036308 (2008).
[26] Y. Yang, J. Elgeti, and G. Gompper, Phys. Rev. E **78**, 061903 (2008).
[27] E. E. Keaveny and M. R. Maxey, Phys. Rev. E **77**, 041910 (2008).
[28] P. T. Underhill, J. P. Hernandez-Ortiz, and M. D. Graham, Phys. Rev. Lett. **100**, 248101 (2008).
[29] U. Erdmann and W. Ebeling, Fluct. Noise Lett. **3**, L145 (2003).
[30] A. Baskaran and M. C. Marchetti, Phys. Rev. Lett. **101**, 268101 (2008).
[31] A. Baule, K. V. Kumar, and S. Ramaswamy, J. Stat. Mech.: Theory Exp. (2008) P11008.
[32] S. van Teeffelen and H. Löwen, Phys. Rev. E **78**, 020101(R) (2008).

[33] V. Lobaskin, D. Lobaskin, and I. Kulic, Eur. J. Phys. Spec. Top. **157**, 149 (2008).
[34] T. J. Murphy and J. L. Aguirre, J. Chem. Phys. **57**, 2098 (1972).
[35] M. Bixon, Annu. Rev. Phys. Chem. **27**, 65 (1976).
[36] B. Dünweg and J. C. Ladd, *Advanced Computer Simulation Approaches for Soft Matter Sciences III* (Springer, Berlin, Heidelberg, 2009), Vol. 221, pp. 89–166.
[37] B. Liu and B. Dünweg, J. Chem. Phys. **118**, 8061 (2003).
[38] B. Guirao and J. F. Joanny, Biophys. J. **92**, 1900 (2007).
[39] P. S. Lovely and F. W. Dahlquist, J. Theor. Biol. **50**, 477 (1975).
[40] C. W. Oseen, *Neuere Methoden und Ergebnisse in der Hydrodynamik* (Akademischer Verlag, Leipzig, 1927).
[41] J. Happel and H. Brenner, *Low Reynolds Number Hydrodynamics, International Series in the Physical and Chemical Engineering Sciences* (Prentice-Hall, Inc., Englewood Cliffs, N.J., 1965).
[42] R. Zwanzig, J. Kiefer, and G. H. Weiss, Proc. Natl. Acad. Sci. U.S.A. **60**, 381 (1968).
[43] J. Rotne and S. Prager, J. Chem. Phys. **50**, 4831 (1969).
[44] P. Mazur, Physica **110A**, 128 (1982).
[45] P. Mazur and W. van Saarloos, Physica **115A**, 21 (1982).
[46] H. Yamakawa, J. Chem. Phys. **53**, 436 (1970).
[47] T. Ishikawa, M. P. Simmonds, and T. J. Pedley, J. Fluid Mech. **568**, 119 (2006).
[48] E. Wajnryb, P. Szymczak, and B. Cichocki, Physica A **335**, 339 (2004).
[49] P. Hänggi and H. Thomas, Phys. Rep. **88**, 207 (1982).
[50] R. Golestanian, T. B. Liverpool, and A. Ajdari, New J. Phys. **9**, 126 (2007).
[51] T. Ishikawa and T. J. Pedley, J. Fluid Mech. **588**, 437 (2007).
[52] T. Ishikawa, J. T. Locsei, and T. J. Pedley, J. Fluid Mech. **615**, 401 (2008).
[53] J.-C. Meiners and S. R. Quake, Phys. Rev. Lett. **82**, 2211 (1999).
[54] M. Polin, D. G. Grier, and S. R. Quake, Phys. Rev. Lett. **96**, 088101 (2006).
[55] R. D. Astumian and P. Hänggi, Phys. Today **55**(11), 33 (2002).
[56] R. Golestanian, Eur. Phys. J. E **25**, 1 (2008).
[57] J. Dunkel and P. Hänggi, Phys. Rep. **471**, 1 (2009).